Research Paper

Effects of Ultrasonic Power and Intensity of Mechanical Agitation on Pretreatment of a Gold-Bearing Arsenopyrite

Won Chol HONG*, Ye Yong KIM, Chang Dok KWON, Kwang Chol SO

Faculty of Mining Engineering
Kim Chaek University of Technology
Democratic People's Republic of Korea

*Corresponding Author e-mail: hwc89217@star-co.net.kp

In this paper, the effects of an ultrasonic power and the intensity of mechanical agitation for pulp on alkaline pretreatment of gold-bearing arsenopyrite were investigated. The effect of pulp temperature on leaching efficiency in alkaline pretreatment of arsenopyrite was investigated under ultrasound and non-ultrasound conditions. Pre-treatment was followed by gold leaching tests with a cyanide solution. Compared with the non-ultrasound condition at the temperature of 60 °C, arsenic extraction and gold extraction was increased 20 %, 14.4 %, respectively, in the presence of ultrasound at ambient temperature. The characteristics of the ultrasonic power level as a function of the intensity of mechanical agitation were evaluated by a numerical simulation with CFD software – Ansys Fluent. The simulation results demonstrated that the stronger intensity of mechanical agitation, the lower ultrasonic power level. These results were proved through leaching experiments at different rotation speeds of impeller and ultrasonic powers.

The study results demonstrate that the ultrasound is an effective factor for pretreatment of gold bearing arsenopyrite and gold extraction is related to an ultrasonic power and the intensity of mechanical agitation.

Keywords: gold; arsenopyrite; alkaline pretreatment; ultrasound; computational fluid dynamics (CFD); Ansys Fluent.

1. Introduction

The refractory gold ore means the mineral of which gold extractions are less than 80 % after fine grinding using a traditional cyanide leaching (La Brooy *et al.*, 1994). Commonly, arsenic-bearing gold ore is very refractory. Gold exists in the form of ultrafine particles or microscopic lattice within arsenic mineral in these ores, so it cannot attach to cyanide during the cyanide leaching process (Mesa Espitia, Lapidus, 2015). Therefore, it is necessary to break these ores up to the gold particle size or decompose to make gold exposed before leaching (Chryssoulis, McMullen, 2005; Deng, Gu, 2018; Hashemzade-hfini *et al.*, 2011). The process such as decomposition and crushing prior to leaching is called the pretreatment of refractory gold ore. The pretreatment is significant in the leaching of gold bearing arsenopy-

rite (Corkhill, Vaughan, 2009). Recently, many researchers have studied the pretreatment of a gold bearing arsenopyrite to expose gold and remove arsenic by changing mineral composition, electrochemical and physicochemical properties of the gold ore (Nan *et al.*, 2014). There are many pretreatment methods of refractory gold ores including roasting oxidation, bacterial oxidation, pressure oxidation and chemical pretreatment. Particularly, the chemical treatment is widely used due to its low cost (Dang *et al.*, 2016). The typical methods for the chemical pretreatment include alkaline pretreatment, acid treatment, wet chlorination, and HNO_3 catalyzing oxidation decomposition. However, the alkaline pretreatment is considered as the most economical and eco-friendly (Meng *et al.*, 2003; Mikhlin *et al.*, 2006). Bhakta *et al.* (1989) developed the alkaline pretreatment of gold bearing arsenopyrite on the basis of previous literatures. This process needs

low potential for oxidizing gold bearing arsenopyrite on alkaline medium:

$$2\text{FeAsS} + 10\text{OH}^- + 7\text{O}_2 = \text{Fe}_2\text{O}_3 + 2\text{AsO}_4$$
$$+ 2\text{SO}_4^{2-} + 5\text{H}_2\text{O}. \quad (1)$$
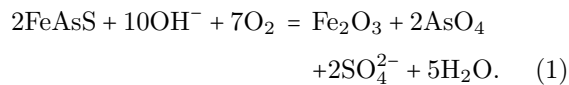
They found that the iron oxide film was hydrated and transferred into the porous state when sodium hydroxide was used. They also found that temperature was very significant. Awe and Sandström (2010) pretreated a tetrahedrite-rich complex ore using selective dissolution of arsenic and antimony. The extraction ratio was related to the concentration of sulphur and hydroxide, temperature and reaction time. Meng *et al.* (2003) investigated to increase gold extraction in the leaching of arsenic-bearing gold ores. They confirmed that gold was separated from sulphur and arsenic in the concentrate when the alkaline pretreatment was applied to it in the conditions of ambient temperature and pressure after ultra-grinding. This method is not widely used due to the dependence of the alkaline pretreatment on alkaline concentration, temperature and pressure.

Recently, the ultrasound has been widely used to accelerate the speed of chemical reaction (Contamine *et al.*, 1994). Unlike microwave, electrochemical and photochemical processing, all it needs is the medium for its transmission. Ultrasound can break down cavitation bubbles near the heterogeneous solid-liquid interface prior to generation of asymmetric flow and liquid jet. It can increase mass and heat transformation due to the breakdown of boundary layers. Collision between particles can occur corrosion and washing of a solid surface and decrease wettability. Ultrasound can cause a weak flow of the solid-liquid boundary surface and reduce the diffusion thickness. It can accelerate the diffusion speed to increase extraction. Many researchers have already studied the gold extraction using ultrasound (Zhu *et al.*, 2012), the effect of ultrasound on zinc extraction (Slaczka, 1986), the effect of ultrasound on copper extraction from copper ore (Bese, 2007; Wang *et al.*, 2017), the effect of ultrasound on leaching of phosphate using hydrochloric acid (Tekin, 2002), and the effect of ultrasound on sulfuric acid leaching of colemanite (Taylan *et al.*, 2007).

As the application range of ultrasound broadens, many studies have been made for analyzing fluid dynamic characteristics as a function of ultrasound parameters during leaching combined ultrasound such as size distributions and energy levels of cavitation bubbles as functions of power and frequency of ultrasound (Merouani *et al.*, 2014; Müller *et al.*, 2014), change of the characteristics of fluid flow due to ultrasound and mechanical agitation (Sajjadi *et al.*, 2015; Kojima *et al.*, 2010). However, the effects of ultrasonic power and intensity of mechanical agitation on leaching of minerals are rarely involved.

Therefore, an investigation concerning the effect of ultrasound and the relation between ultrasonic power and intensity of mechanical agitation was conducted by computational fluid dynamics simulation and experiments.

2. Experimental

2.1. Materials

The refractory gold bearing arsenopyrite was obtained from DokSong Mine, Democratic People's Republic of Korea. The arsenopyrite samples with a particle size – 0.074 mm were used in all experiments. The chemical composition of material is given in Table 1. The samples were crushed, ground, and then sieved using ASTM standard sieves.

Table 1. Composition analysis result.

Elements	Amount [%]
Au ($\times 10^{-6}$)	19.87
Ag ($\times 10^{-6}$)	1.44
As	41.53
Fe	35.51
S	20.21
SiO$_2$	2.49
Al$_2$O$_3$	0.13
CaO	0.05
MgO	0.08

2.2. Experimental methods

The experiments were conducted in three stages.

In the first stage, gold bearing arsenopyrite was pre-leached using alkali. This experiment was carried out in 1000 ml beaker placed in the thermostatic bath within a precision of ±0.1 °C, using a mechanical agitator (LR500A, Yamato Scientific Co., Ltd., Japan) and hydraulic ultrasonic generator (GuangZhou Hengda Ultrasonic Electric Technological Ltd., China) with the power adjustable in the range of 0 W–150 W and 20 kHz frequency, 200 g arsenopyrite sample, and 800 ml distilled water were introduced into the experimental beaker equipped with the ultrasonic probe and thermometer. After that, 20 g sodium hydroxide (analytically pure) was put into the solution and mechanically stirred for 6 h at 350 rpm at different temperatures (20 °C, 40 °C, 60 °C, and 80 °C) without ultrasound. Then, it was stirred for 6 h at 20 °C in the presence of ultrasound. While these experiments were carried out, leaching pulps were taken and filtered at the time intervals of 1 h to survey arsenic extraction using atomic absorption spectrometer (model Varian SpectrAA 220FS). After the alkaline pretreatment, the pulp was filtered, washed with distilled water three

times and then the residue was dried at 120 °C. Dried residues were used in the next stage of experiments.

In the second stage, the pretreated arsenopyrite samples were leached using sodium cyanide; 150 g pretreated sample and 600 ml distilled water were poured into the beaker. The pulp was mechanically stirred at 600 rpm, at room temperature. The pH of solution was adjusted to 10.5~11 using sodium hydroxide. Then, 1.2 g chemically pure sodium cyanide was added to the pulp. In other words, the consumption of sodium cyanide is 8 kg/t on plant scale. The leaching was conducted for 8 h. At the time intervals of 1 h, pulps were taken and filtered to survey gold extraction. The concentration of gold in pulp was analyzed using an atomic absorption spectrometer (model Varian SpectrAA 220FS).

In the third stage, the relation between ultrasonic power and intensity of mechanical agitation was analyzed by computational fluid dynamic simulation and experiments. For analyzing transmission characteristics of ultrasonic power, unsteady LES (large eddy simulation) model and FW-H (Ffows-Williams & Hawkings) model were used. Based on the simulation result, the arsenic and gold extractions were compared as a function of time by varying the ultrasonic power (150 W, 400 W, 1000 W) and agitation intensity (150 rpm, 350 rpm, 550 rpm, 750 rpm).
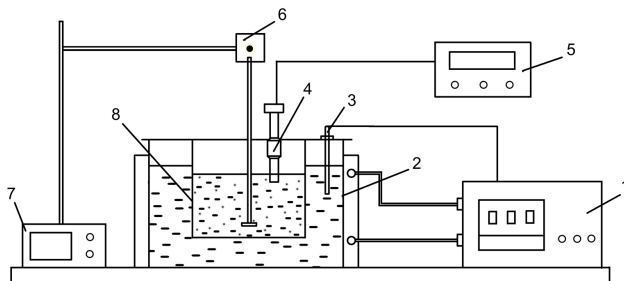
The experimental set-up is shown in Fig. 1.

Fig. 1. Schematic experimental set-up; 1) thermostat; 2) thermostatic bath; 3) thermometer; 4) ultrasonic generator; 5) hydraulic pump; 6) mechanical agitator; 7) agitator controller; 8) beaker.

3. Results and discussions

3.1. Effect of ultrasound on alkaline pretreatment

The effect of ultrasound on the alkaline pretreatment of gold-bearing arsenopyrite was shown in Figs. 2 and 3.

As shown in Fig. 2, the temperature of pulp had a great influence on leaching dynamics under no ultrasound. The arsenic extraction increased as the temperature increased. However, the initial extraction was significantly high at 80 °C, after 5 h it became lower than the one at 60 °C. Under ultrasound condition, arsenic extraction was a little lower than the one without ultra-
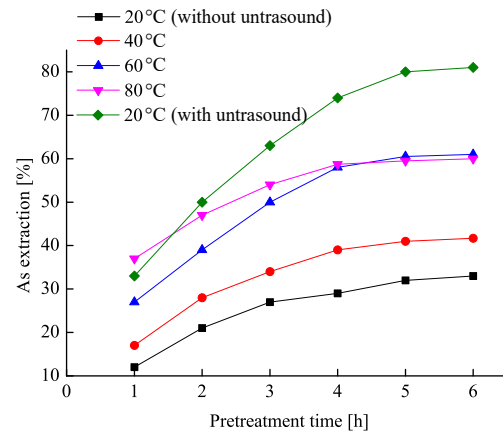

Fig. 2. Arsenic extractions with and without ultrasound on alkaline pretreatment.
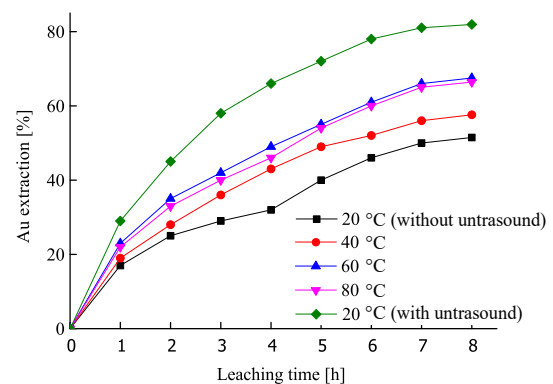

Fig. 3. Gold extractions with and without ultrasound on alkaline pretreatment.

sound at 1 h and it increased 20 % more than the one without ultrasound at the end of leaching. This indicates that ultrasound has a great influence on leaching dynamics. Due to the cavitation, the extremely high temperature and pressure are provided on the interface between solution and solid matrix. PENN *et al.* (1959) found that ultrasound wave reduced the thickness of boundary layer for the mass transfer, thus facilitating the mass transfer.

Figure 3 shows that the gold extraction in cyanidation was in proportion to arsenic extraction.

3.2. Relation between ultrasonic power and intensity of mechanical agitation on alkaline pretreatment

3.2.1. Computational fluid dynamics simulation

3.2.1.1. Modeling for the simulation. Acronyms:

r – radial coordinates of the receiver location,

$I(r, \theta; \mathbf{y})$ – directional ultrasonic intensity per unit volume of a jet,

C – modified convection factor,

u – turbulence velocity,
M – dimensionless parameter,
N – dimensionless parameter,
k – turbulence kinetic energy,
P_A – total ultrasonic power,
P_{ref} – reference ultrasonic power,
θ – angular coordinates of the receiver location,
ϵ – turbulence dissipation rate.

The Jet Noise Source model was proposed by Goldstein and Ribner who modified the model originally defined by Ribner. It is considered for anisotropy of turbulence in axisymmetric turbulent jets.

Goldstein proposed that the total ultrasonic power emitted by the unit volume of a turbulent jet is calculated from:

$$P_A(\mathbf{y}) = \int\limits_{2\pi}^{0} \int\limits_{\pi}^{0} I(r,\theta;\mathbf{y}) r^2 \sin\theta \, \mathrm{d}\theta \, \mathrm{d}\psi$$

$$= 2\pi r^2 \int\limits_{\pi}^{0} I(r,\theta;\mathbf{y}) \sin\theta \, \mathrm{d}\theta, \tag{2}$$

where r and θ are the radial and angular coordinates of the receiver location, and $I(r,\theta;\mathbf{y})$ is the directional ultrasonic intensity per unit volume of a jet defined by:

$$I(r,\theta;\mathbf{y}) = \frac{12\rho_0 \omega_f^4 L_1 L_2 \overline{u_{t1}^2}^2}{5\pi a_0^5 r^2} \frac{D_{\text{self}}}{C^5}$$

$$+ \frac{24\rho_0 \omega_f^4 L_1 L_2^4 \overline{u_{t1}^2}}{\pi a_0^5 r^2} \left(\frac{\partial U}{\partial r}\right)^2 \frac{D_{\text{shear}}}{C^5}. \tag{3}$$

C is the modified convection factor defined as:

$$C = 1 - M_c \cos\theta \tag{4}$$

and

$$D_{\text{self}} = 1 + 2\left(\frac{M}{9} - N\right)\cos^2\theta \sin^2\theta$$

$$+ \frac{1}{3}\left[\frac{M^2}{7} + M - 1.5N\left(3 - 3N + \frac{1.5}{\Delta^2} - \frac{\Delta^2}{2}\right)\right]\sin^4\theta, \tag{5}$$

$$D_{\text{shear}} = \cos^2\theta\left[\cos^2\theta + \frac{1}{2}\left(\frac{1}{\Delta^2} - 2N\right)\sin^2\theta\right]. \tag{6}$$

The other parameters are defined by:

$$\Delta = \frac{L_2}{L_1}, \tag{7}$$

$$M = \left[\frac{3}{2}\left(\Delta - \frac{1}{\Delta}\right)\right]^2, \tag{8}$$

$$N = 1 - \frac{\left(\overline{u_{t2}^2}\right)}{\left(\overline{u_{t1}^2}\right)}, \tag{9}$$

$$L_1 = \frac{\left(\overline{u_{t1}^2}\right)^{1.5}}{\epsilon}, \tag{10}$$

$$L_2 = \frac{\left(\overline{u_{t2}^2}\right)^{1.5}}{\epsilon}, \tag{11}$$

$$\omega_f = 2\pi\frac{\epsilon}{k}, \tag{12}$$

where $\overline{u_{t1}^2}$ and $\overline{u_{t2}^2}$ are computed, respectively, according to the turbulence model chosen for computing. If the RSM is selected, they are computed from the corresponding normal stresses. For all other two-equation turbulence models, they are calculated from:

$$\overline{u_{t1}^2} = \frac{8}{9}k, \tag{13}$$

$$\overline{u_{t2}^2} = \frac{4}{9}k. \tag{14}$$

In Ansys Fluent (2016), the ultrasonic power both in the dimensional units and dB is computed from:

$$L_P = 10\log\left(\frac{P_A}{P_{\text{ref}}}\right), \tag{15}$$

where P_{ref} is the reference ultrasonic power ($P_{\text{ref}} = 10^{-12}$ W by default).

3.2.1.2. Model structure. Model of mechanical agitator equipped ultrasonic generator is as shown in Fig. 4.
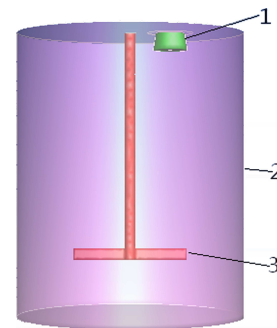

Fig. 4. Model of mechanical agitator equipped ultrasonic generator: 1) ultrasonic generator; 2) agitator box; 3) agitator impeller.

The unstructured mesh of a mechanical agitator equipped with an ultrasonic generator was created in Ansys ICEM. The model domain was discretized into 583.742 hexahedral elements and tetrahedral elements, 964.532 nodes.

Figure 5 shows the mesh model structure of mechanical agitator equipped with an ultrasonic generator. The model was meshed in minimum size 0.5 mm (around ultrasonic probe) and the stability of the mesh is performed by check of mesh.

Base data to create calculation structure was determined such as experimental conditions for simulation analysis (Table 2).
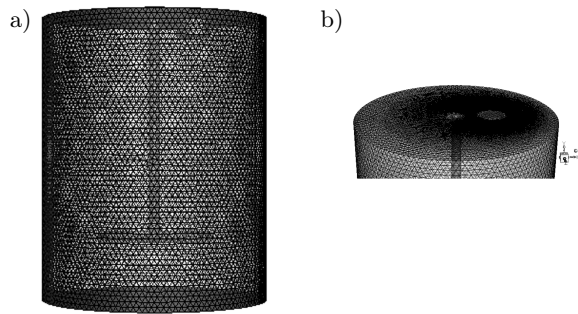
a)

b)

Fig. 5. Computational domain of model: a) computational domain of mechanical agitator modeling; b) computational domain of regions around ultrasonic generator.

Table 2. Data to create calculation structure.

Data	Value
Dimension of calculation region	3
Dimension of ultrasonic generation region	1
Dimension of agitation region	1
Size of agitator's impeller [mm]	200
Maximum mesh scale [mm]	10
Minimum mesh scale [mm]	0.5
Dimension of calculation region [mm × mm]	$\varnothing 400 \times 500$
Number of phase	1

3.2.1.3. Calculation condition. Boundary conditions for simulation analysis were shown in Table 3.

Table 3. Calculation condition.

Classification	Data	Unit	Value
Boundary condition	Ultrasonic power	W	150, 400, 1000
	Frequency	Hz	20000
	Temperature	K	293
	Agitation intensity	rpm	150, 350, 550, 750
	Chemical composition	–	Water
Calculation model	RSM model		
	Abnormal problem		

3.2.1.4. Simulation results. The effect of agitation intensity on an ultrasonic power was analyzed using the CFD simulation while varying agitation intensity.

Firstly, the ultrasonic power level as a function of agitation intensity was investigated under ultrasonic power of 150 W. That result was shown in Figs. 6 and 7.

Based on the simulation result, the attenuation ratio which reflects the change of ultrasonic power, was investigated at 25 cm apart from the bottom of beaker on the axis of oscillator. That result was shown in Fig. 8.

As shown in Fig. 8, the ultrasonic power level decreases as agitation intensity increases. For the agitation speeds of 150 rpm, 350 rpm, 550 rpm, 750 rpm, the attenuation ratios were 55.1 %, 60.2 %, 68.0 %, 75.8 %, respectively.
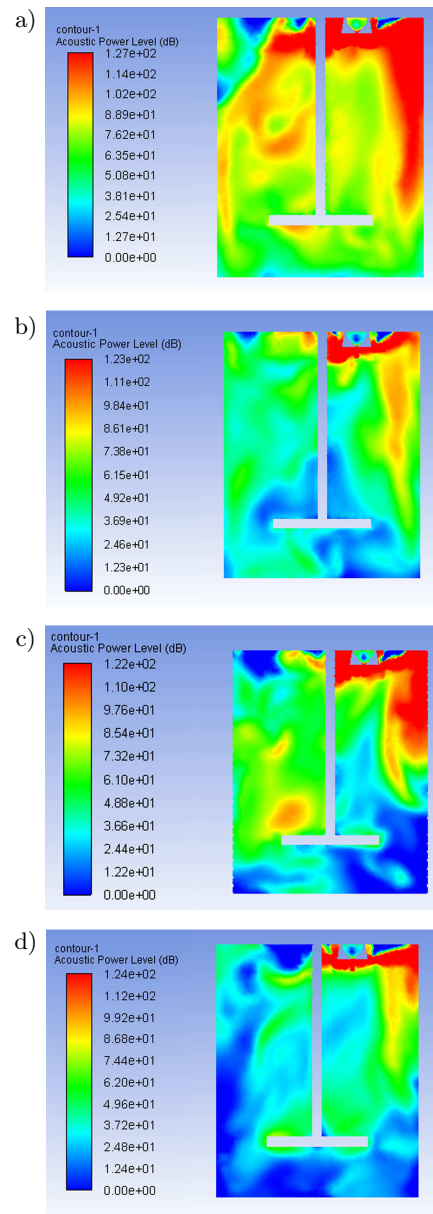
a)

b)

c)

d)

Fig. 6. Distribution character of acoustic power level according to the different agitation intensity under ultrasonic power of 150 W: a) 150 rpm; b) 350 rpm; c) 550 rpm; d) 750 rpm.

Next, the ultrasonic power level as a function of agitation intensity was also investigated under an ultrasonic power of 400 W. That result was shown in Figs. 9 and 10.

Similarly, the attenuation ratio of an ultrasonic power as a function of agitation speed was shown in Fig. 11.

As shown in Fig. 11, at the agitation speeds of 150 rpm, 350 rpm, 550 rpm, 750 rpm, the attenuation ratios were 41.8 %, 47.3 %, 56.3 %, 63.5 %, respectively.

Finally, the ultrasonic power level as a function of agitation intensity was also investigated under an ul-
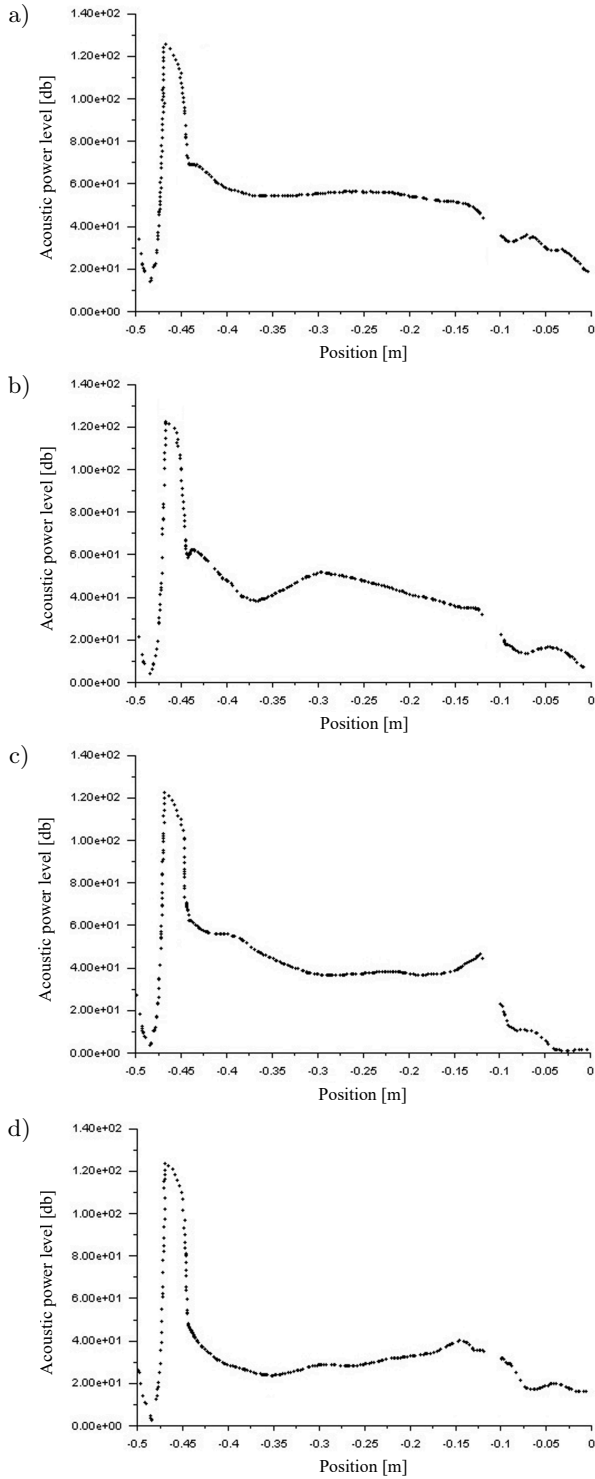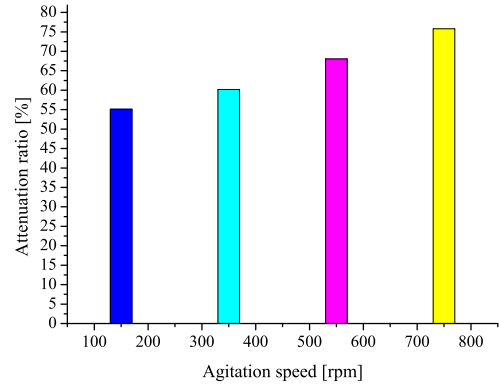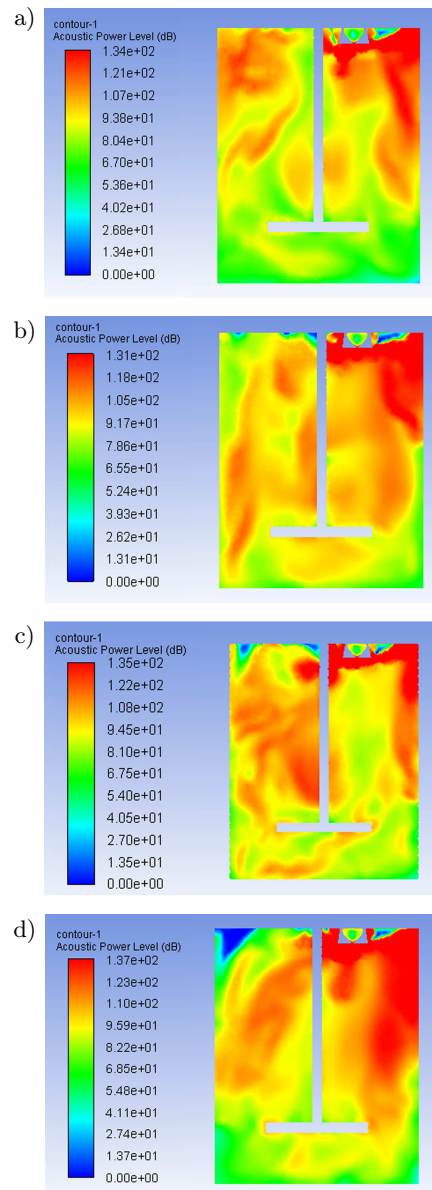
a)

b)

c)

d)

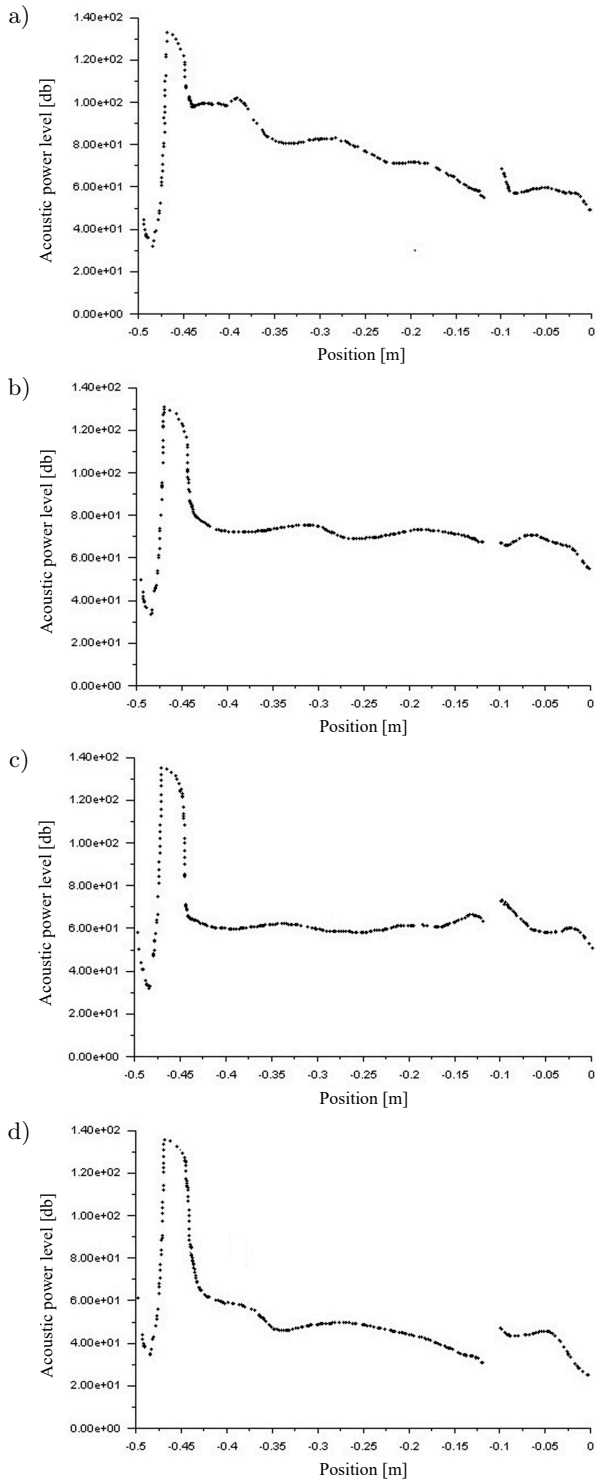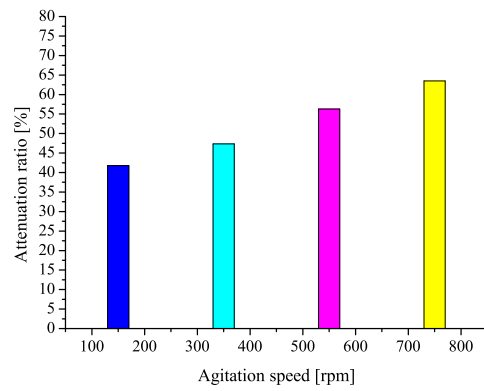
Fig. 7. Characteristic curve of acoustic power level according to the distance from agitator's bottom under ultrasonic power of 150 W: a) 150 rpm; b) 350 rpm; c) 550 rpm; d) 750 rpm.

Fig. 8. Attenuation ratio of acoustic power level according to the different agitation intensity under ultrasonic power of 150 W.
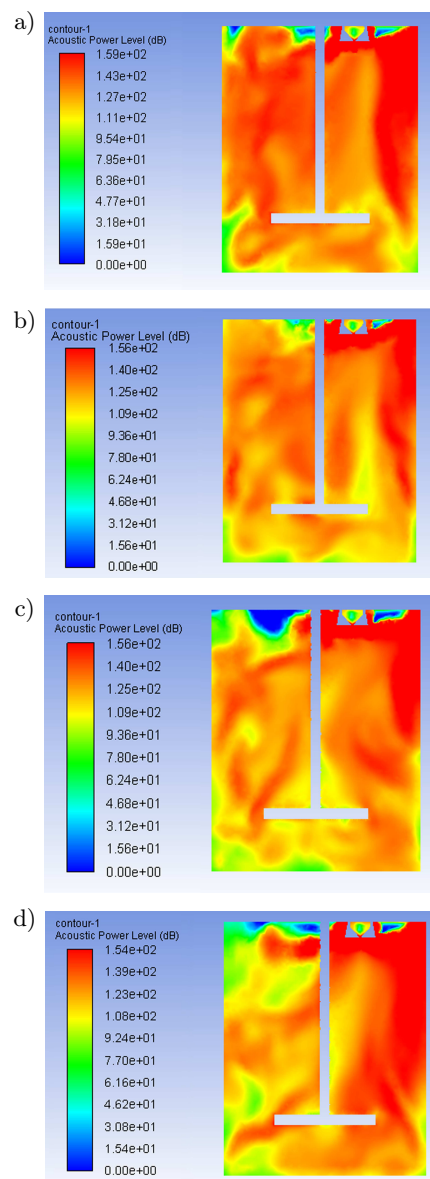
a)

b)

c)

d)

Fig. 9. Distribution character of acoustic power level according to the different agitation intensity under an ultrasonic power of 400 W: a) 150 rpm; b) 350 rpm; c) 550 rpm; d) 750 rpm.

trasonic power of 1000 W. That result was shown in Figs. 12 and 13.

Similarly, the attenuation ratio of the ultrasonic power level as a function of agitation speed was shown in Fig. 14.

a)

b)

c)

d)

Fig. 10. Characteristic curve of acoustic power level according to the distance from agitator's bottom under ultrasonic power of 400 W: a) 150 rpm; b) 350 rpm; c) 550 rpm; d) 750 rpm.

Fig. 11. Attenuation ratio of acoustic power level according to the different agitation intensity under ultrasonic power of 400 W.

a)

b)

c)

d)

Fig. 12. Distribution character of acoustic power level according to the different agitation intensity under ultrasonic power of 1000 W: a) 150 rpm; b) 350 rpm; c) 550 rpm; d) 750 rpm.
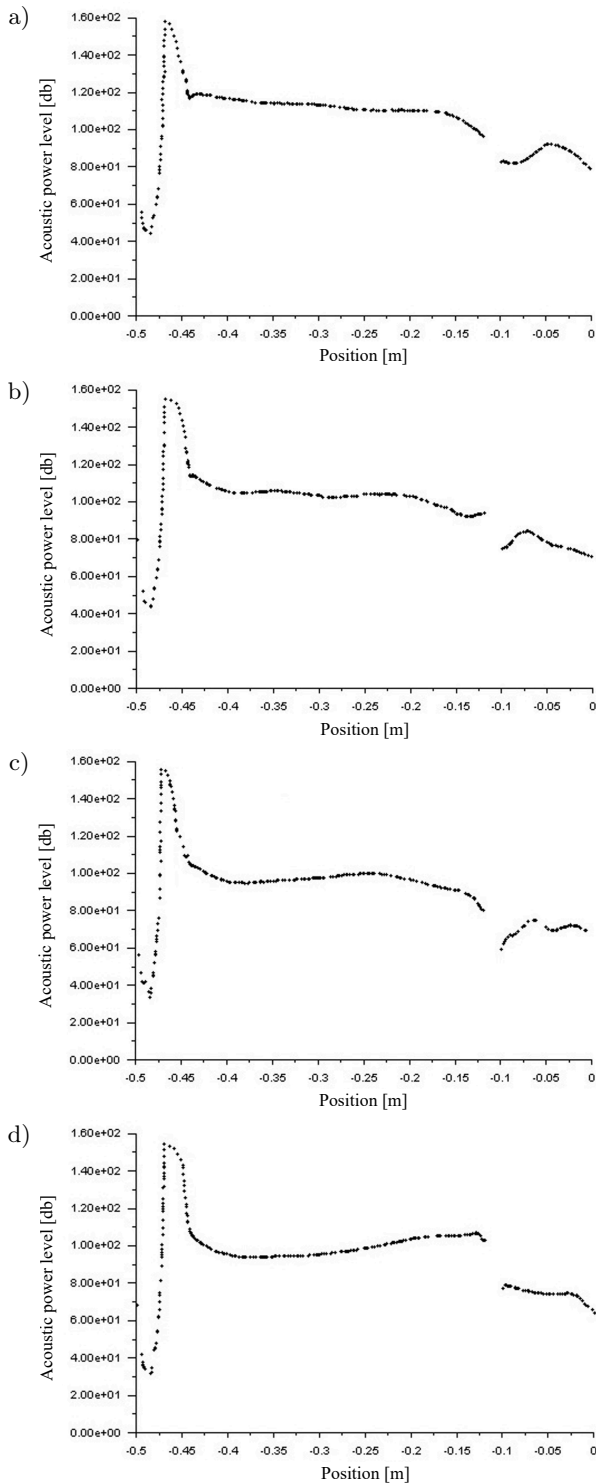
As shown in Fig. 14, for the agitation speeds of 150 rpm, 350 rpm, 550 rpm, 750 rpm, the attenuation ratios were 29.6 %, 32.0 %, 35.3 %, 35.1 %, respectively.

a)

b)

c)

d)

Fig. 13. Characteristic curve of acoustic power level according to the distance from agitator's bottom
under ultrasonic power of 1000 W: a) 150 rpm; b) 350 rpm; c) 550 rpm; d) 750 rpm.

The simulation results show that an ultrasonic power decreases as agitation intensity increases. Besides, it also demonstrated that the detrimental effect of intensity of mechanical agitation decreased as an ultrasonic power increased.
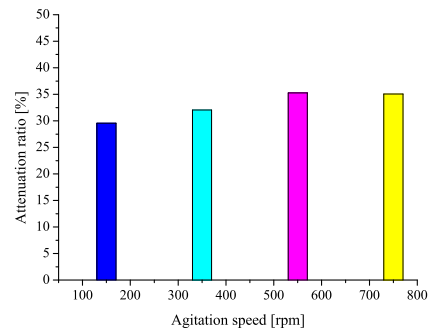

Fig. 14. Attenuation ratio of acoustic power level according to the different agitation intensity under ultrasonic power of 1000 W.

3.2.2. Experimental results

Based on the simulation results, experiments were carried out for proving them.

Relations between an ultrasonic power and agitation intensity on the alkaline pretreatment were shown in Figs. 15–17.

Figure 15 shows the effect of agitation intensity under an ultrasonic power of 150 W.

As shown in Fig. 15, when agitation intensity increased from 150 rpm to 350 rpm under an ultrasonic power of 150 W, arsenic extraction increased more and more. Also, the initial arsenic extraction rate was high at 550 rpm during 3 h after starting leaching under ultrasound, but it decreased again afterwards. The extraction of arsenic was higher at 350 rpm than that at
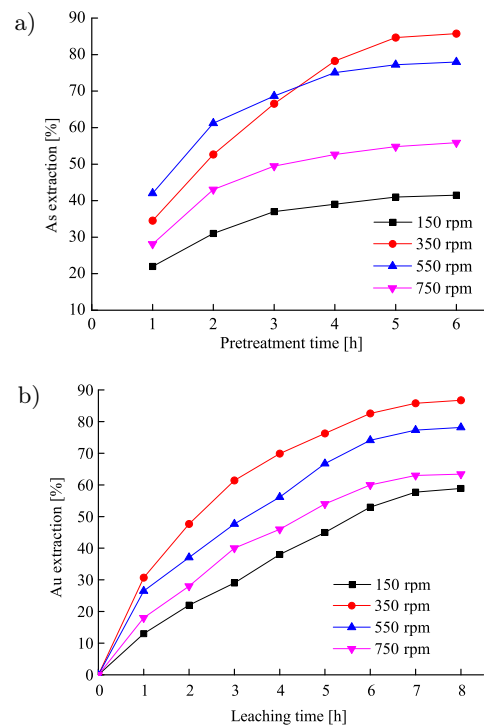
a)

b)

Fig. 15. Effect of agitation intensity under ultrasonic power of 150 W: a) arsenic extraction; b) gold extraction.
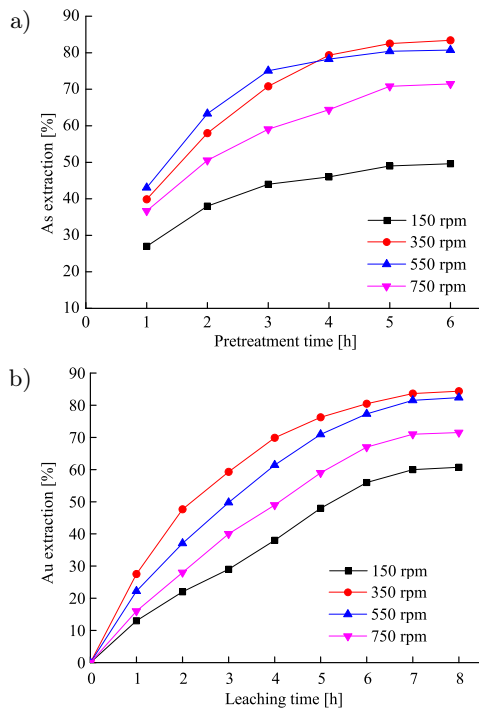
Fig. 16. Effect of agitation intensity under ultrasonic power of 400 W: a) arsenic extraction; b) gold extraction.
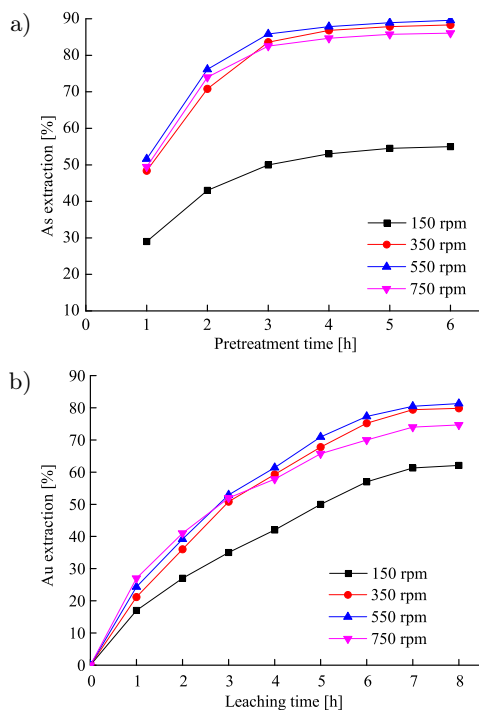

Fig. 17. Effect of agitation intensity under ultrasonic power of 1000 W: a) arsenic extraction; b) gold extraction.

750 rpm. This indicates that the maximum of extraction is available at 350 rpm under an ultrasonic power of 150 W. The extraction of gold in the pretreated sample might be proportional to the arsenic extraction.

As shown in Fig. 16, the extraction of arsenic increased as the agitation intensity increased from 150 rpm to 550 rpm under an ultrasonic power of 400 W. When the pretreated sample was leached for 5 h under ultrasound, the extraction of arsenic was 1 % lower at 550 rpm than the one at 350 rpm. This shows that the agitation intensity had influence on the extraction of arsenic unlike an ultrasonic power of 150 W.

The arsenic extraction was 67 % at agitation intensity of 750 rpm at leaching time of 6 h. It was higher than that at 150 W. But the extraction of arsenic and gold were also the highest at 350 rpm.

Figure 17 shows the effect of agitation intensity under ultrasonic power of 1000 W. As shown in Fig. 17, when agitation intensity changed from 150 rpm to 550 rpm, the arsenic extraction increased. The extraction of arsenic at 750 rpm was 28.3 %, 13.7 % higher than that at 150 W and 400 rpm. Therefore, it can be thought that the detrimental effect of agitation intensity decreased with the increase of an ultrasonic power. In this case, the extraction of gold was not proportional to the arsenic extraction. It could be attributed to the acceleration of a formation of SiO_2 gel and adsorption of gold in pulp to it due to a high ultrasonic power (Zhang *et al.*, 2016).

At the agitation speed of 150 rpm, an ultrasonic power was attenuated least from the simulation, whereas the extractions of arsenic and gold were lowest. It attributes to the settling of mineral particles onto the bottom due to the low agitation speed. But both results from experiment and simulation were consistent at different agitation speeds.

4. Conclusions

Arsenic and gold extractions at 60 °C were 61 % and 67.5 %, respectively, without ultrasound, whereas 81 % and 81.9 % at 20 °C with ultrasound. This shows that ultrasound might be favourable for an alkaline pretreatment of gold bearing arsenopyrite.

Through CFD simulation, it was demonstrated that an ultrasonic power decreased as intensity of mechanical agitation increased, and the detrimental effect of mechanical stirring decreased as an ultrasonic power increased.

The experiment results showed that the gold extraction was the highest at 150 W and 350 rpm. These results showed that the proper ultrasonic power and agitation intensity should be selected on the pretreatment of gold-bearing arsenopyrite and the ultrasonic power could be interfered with agitation intensity. But, the interference decreased with the increase of an ultrasonic power.

References

1. Ansys Fluent (2016), User's guide manual fluent Inc., Ansys Fluent 16.0, Pittsburgh, USA.

2. Awe S., Sandström Å. (2010), Selective leaching of arsenic and antimony from a tetrahedrite rich complex sulphide concentrate using alkaline sulphide solution, *Minerals Engineering*, **23**(15): 1227–1236, doi: 10.1016/j.mineng.2010.08.018.

3. Bese A.V. (2007), Effect of ultrasound on the dissolution of copper from copper converter slag by acid leaching, *Ultrasonics Sonochemistry*, **14**(6): 790–796, doi: 10.1016/j.ultsonch.2007.01.007.

4. Bhakta P., Langhans J., Lei K. (1989), *Alkaline oxidative leaching of gold-bearing arsenopyrite ores*, Report of Investigations 9258, Bureau of Mines, United States Department of the Interior, p. 1–11.

5. Chryssoulis S.L., McMullen J. (2005), Mineralogical investigation of gold ores, *Developments in Mineral Processing*, **15**: 21–71, doi: 10.1016/S0167-4528(05)15002-9.

6. Contamine F., Faid F., Wilhelm A.M., Berlan J., Delmas H. (1994), Chemical reactions under ultrasound: discrimination of chemical and physical effects, *Chemical Engineering Science*, **49**(24, Part 2): 5865–5873, doi: 10.1016/0009-2509(94)00297-5.

7. Corkhill C.L., Vaughan D.J. (2009), Arsenopyrite oxidation – A review, *Applied Geochemistry*, **24**(12): 2342–2361, doi: 10.1016/j.apgeochem.2009.09.008.

8. Dang X. Ke W., Tang C., Lv J., Zhou X., Liu C. (2016), Increasing leaching rate of gold cyanide of two-stage calcination generated from refractory ore containing arsenopyrite and pyrrhotite, *Rare Metals*, **35**(10): 804–810, doi: 10.1007/s12598-015-0470-0.

9. Deng S., Gu G. (2018), An electrochemical impedance spectroscopy study of arsenopyrite oxidation in the presence of Sulfobacillus thermosulfidooxidans, *Electrochimica Acta*, **287**: 106–114, doi: 10.1016/j.electacta.2018.08.051.

10. Hashemzadehfini M., Ficeriová J., Abkhoshk E., Shahraki B. (2011), Effect of mechanical activation on thiosulphate leaching of gold from complex sulfide concentrate, *Transactions of Nonferrous Metals Society of China*, **21**(12): 2744–2751, doi: 10.1016/S1003-6326(11)61118-7.

11. Kojima Y., Asakura Y., Sugiyama G., Koda S. (2010), The effects of ultrasonic flow and mechanical flow on the sonochemical efficiency in a rectangular sonochemical reactor, *Ultrasonics Sonochemistry*, **17**(6): 978–984, doi: 10.1016/j.ultsonch.2009.11.020.

12. La Brooy S.R., Linge H.G., Walker G.S. (1994), Review of gold extraction from ores, *Minerals Engineering*, **7**(10): 1213–1241, doi: 10.1016/0892-6875(94)90114-7.

13. Meng Y., Wu M., Su S., Wang L. (2003), Intensified alkaline leaching pretreatment of refractory gold concentrate at common temperature and pressure [in Chinese], *Transactions of Nonferrous Metals Society of China*, **13**(2): 426–430.

14. Merouani S., Hamdaoui O., Rezgui Y., Guemini M. (2014), Energy analysis during ultrasonic bubble oscillations: Relationship between bubble energy and sonochemical parameters, *Ultrasonics*, **54**(1): 227–232, doi: 10.1016/j.ultras.2013.04.014.

15. Mesa Espitia S.L., Lapidus G.T. (2015), Pretreatment of a refractory arsenopyritic gold ore using hydroxyl ion, *Hydrometallurgy*, **153**: 106–113, doi: 10.1016/j.hydromet.2015.02.013.

16. Mikhlin Y.L., Romanchenko A.S., Asanov I.P. (2006), Oxidation of arsenopyrite and deposition of gold on the oxidized surfaces: A scanning probe microscopy, tunneling spectroscopy and XPS study, *Geochimica et Cosmochimica Acta*, **70**(19): 4874–4888, doi: 10.1016/j.gca.2006.07.021.

17. Müller S., Fischper M., Mottyll S., Skoda R., Hussong J. (2014), Analysis of the cavitating flow induced by an ultrasonic horn – Experimental investigation on the influence of actuation phase, amplitude and geometrical boundary conditions, *EPJ Web of Conferences*, **67**: 02079, doi: 10.1051/epjconf/20146702079.

18. Nan X. Cai X., Kong J. (2014) Pretreatment process on refractory gold ores with As, *ISIJ International*, **54**(3): 543–547, doi: 10.2355/isijinternational.54.543.

19. Penn R., Yeager E., Hovorka F. (1959), The effect of ultrasonic waves on the dissolution of Nickel, *Journal of the Acoustical Society of America*, **31**: 1372–1376.

20. Sajjadi B., Raman A.A.A., Ibrahim S. (2015), A comparative fluid flow characterisation in a low frequency/high power sonoreactor and mechanical stirred vessel, *Ultrasonics Sonochemistry*, **27**: 359–373, doi: 10.1016/j.ultsonch.2015.04.034.

21. Slaczka A.St. (1986), Effect of ultrasound on ammonium leaching of zinc from galmei ore, *Ultrasonics*, **24**(1): 53–55, doi: 10.1016/0041-624X(86)90075-2.

22. Taylan N., Gürbüz H., Bulutcu A.N. (2007), Effects of ultrasound on the reaction step of boric acid production process from colemanite, *Ultrasonics Sonochemistry*, **14**(5): 633–638, doi: 10.1016/j.ultsonch.2006.11.001.

23. Tekin T. (2002), Use of ultrasound in the dissolution kinetics of phosphate rock in HCl, *Hydrometallurgy*, **64**(3): 187–192, doi: 10.1016/S0304-386X(02)00040-3.

24. Wang S., Cui W., Zhang G., Zhang L., Peng J. (2017), Ultra fast ultrasound-assisted decopperization from copper anode slime, *Ultrasonics Sonochemistry*, **36**: 20–26, doi: 10.1016/j.ultsonch.2016.11.013.

25. Zhang G., Wang S., Zhang L., Peng J. (2016), Ultrasound-intensified leaching of gold from a refractory ore, *ISIJ International*, **56**(4): 714–718, doi: 10.2355/isijinternational.ISIJINT-2015-476.

26. Zhu P. Zhang X., Li K., Qian G., Zhou M. (2012), Kinetics of leaching refractory gold ores by ultrasonic-assisted electro-chlorination, *International Journal of Minerals, Metallurgy, and Materials*, **19**(6): 473–477, doi: 10.1007/S12613-012-0582-6.